

**A Numerical Investigation on the Response of Load
Relieving Notches Subjected to Shock Wave Loading**

by Cyril L. Williams, Daniel Scheffler, and William Walters

ARL-RP-462

September 2013

A reprint from *Procedia Engineering*, Vol. 58, pp. 453–460, 2013.

NOTICES

Disclaimers

The findings in this report are not to be construed as an official Department of the Army position unless so designated by other authorized documents.

Citation of manufacturer's or trade names does not constitute an official endorsement or approval of the use thereof.

Destroy this report when it is no longer needed. Do not return it to the originator.

Army Research Laboratory

Aberdeen Proving Ground, MD 21005-5066

ARL-RP-462

September 2013

A Numerical Investigation on the Response of Load Relieving Notches Subjected to Shock Wave Loading

Cyril L. Williams, Daniel Scheffler, and William Walters
Weapons and Materials Research Directorate, ARL

A reprint from *Procedia Engineering*, Vol. 58, pp. 453–460, 2013.

REPORT DOCUMENTATION PAGE			Form Approved OMB No. 0704-0188		
Public reporting burden for this collection of information is estimated to average 1 hour per response, including the time for reviewing instructions, searching existing data sources, gathering and maintaining the data needed, and completing and reviewing the collection information. Send comments regarding this burden estimate or any other aspect of this collection of information, including suggestions for reducing the burden, to Department of Defense, Washington Headquarters Services, Directorate for Information Operations and Reports (0704-0188), 1215 Jefferson Davis Highway, Suite 1204, Arlington, VA 22202-4302. Respondents should be aware that notwithstanding any other provision of law, no person shall be subject to any penalty for failing to comply with a collection of information if it does not display a currently valid OMB control number. PLEASE DO NOT RETURN YOUR FORM TO THE ABOVE ADDRESS.					
1. REPORT DATE (DD-MM-YYYY) September 2013		2. REPORT TYPE Reprint		3. DATES COVERED (From - To) 1 January 2009–12 December 2012	
4. TITLE AND SUBTITLE A Numerical Investigation on the Response of Load Relieving Notches Subjected to Shock Wave Loading			5a. CONTRACT NUMBER		
			5b. GRANT NUMBER		
			5c. PROGRAM ELEMENT NUMBER		
6. AUTHOR(S) Cyril L. Williams, Daniel Scheffler, and William Walters			5d. PROJECT NUMBER		
			5e. TASK NUMBER		
			5f. WORK UNIT NUMBER		
7. PERFORMING ORGANIZATION NAME(S) AND ADDRESS(ES) U.S. Army Research Laboratory ATTN: RDRL-WMP-C Aberdeen Proving Ground, MD 21005-5066			8. PERFORMING ORGANIZATION REPORT NUMBER ARL-RP-462		
9. SPONSORING/MONITORING AGENCY NAME(S) AND ADDRESS(ES)			10. SPONSOR/MONITOR'S ACRONYM(S)		
			11. SPONSOR/MONITOR'S REPORT NUMBER(S)		
12. DISTRIBUTION/AVAILABILITY STATEMENT Approved for public release; distribution is unlimited.					
13. SUPPLEMENTARY NOTES A reprint from <i>Procedia Engineering</i> , Vol. 58, pp. 453–460, 2013.					
14. ABSTRACT Hydrocode simulations were conducted to analyze the non-linear response of 1100-O aluminum plates with semi-circular notches. Plates with constant notch depth and notch root radius were loaded (normal to the notch-tip plane) to the same shock stress while the notch spacing was varied. The resulting stress distributions were analyzed at specific locations between adjacent notches and then the maximum tensile stress developed was determined for different notch spacing. The results show that the maximum tensile stress developed in the target material was found to be a function of notch spacing. Contrary to the case for quasi-static loading where a decrease in notch spacing leads to a decrease in maximum stress, it was determined that the resulting maximum tensile stress for the shock wave loading case decreases when the notch spacing is increased. Numerical results obtained were validated using plate impact experiments. A macrocrack was observed in the vicinity of the maximum tensile region for the smallest notch spacing, while no macrocrack was observed for the largest spacing.					
15. SUBJECT TERMS notch, relieve, stress, hydrocode, simulation, plate impact, spall fracture					
16. SECURITY CLASSIFICATION OF:			17. LIMITATION OF ABSTRACT	18. NUMBER OF PAGES	19a. NAME OF RESPONSIBLE PERSON
a. REPORT	b. ABSTRACT	c. THIS PAGE			Cyril L. Williams
Unclassified	Unclassified	Unclassified	UU	14	19b. TELEPHONE NUMBER (Include area code) 410-278-8753

The 12th Hypervelocity Impact Symposium

A Numerical Investigation on the Response of Load Relieving Notches Subjected to Shock Wave Loading

C. Williams*, D. Scheffler, and W. Walters

U.S. Army Research Laboratory, Protection Division, RDRL-WMP, APG, MD 21005-5066

Abstract

Hydrocode simulations were conducted to analyze the non-linear response of 1100-O aluminum plates with semi-circular notches. Plates with constant notch depth and notch root radius were loaded (normal to the notch-tip plane) to the same shock stress while the notch spacing was varied. The resulting stress distributions were analyzed at specific locations between adjacent notches and then the maximum tensile stress developed was determined for different notch spacing. The results show that the maximum tensile stress developed in the target material was found to be a function of notch spacing. Contrary to the case for quasi-static loading where a decrease in notch spacing leads to a decrease in maximum stress, it was determined that the resulting maximum tensile stress for the shock wave loading case decreases when the notch spacing is increased. Numerical results obtained were validated using plate impact experiments. A macrocrack was observed in the vicinity of the maximum tensile region for the smallest notch spacing, while no macrocrack was observed for the largest spacing.

© 2013 The Authors. Published by Elsevier Ltd.

Selection and peer-review under responsibility of the Hypervelocity Impact Society

Keywords: Shock; Numerical; Simulation; Hydrocode; Notch; Spacing;

1. Introduction

The focus of this paper is the non-linear response of load relieving notches subjected to shock wave loading (normal to the notch-tip plane). A thorough understanding of the response of load relieving notches and the resulting stress distribution within a structural member is of utmost importance to engineers. Such knowledge is directly applicable in the design of long rods and a large variety of structures for which notches are exposed to shock wave loading. Neuber [1], Peterson [2], Arola and Williams [3], Mow and Pao [4], Nakayama et al. [5], Steinchen [6], Shea [7], Niethhammer et al. [8], and many other researchers have studied the effect of single and multiple notches under quasi-static and dynamic loading conditions. However, not much work has been done on load relieving notches subjected to shock wave loading. With advances in hydrocodes over the past two decades, accurate analysis can be performed more efficiently and cost effectively as compared to experimentation.

Bores, grooves, and abrupt changes in a structural member can give rise to stress concentration. The basic concept of stress concentration as described by Neuber [1] is adopted here. For instance, when a bar without a surface notch is loaded in uniaxial tension as shown in Fig. 1(a), a uniform stress distribution prevails. However, if a symmetrical surface notch is cut into both sides of an identical bar and loaded in uniaxial tension as shown in Fig. 1(b), the stress distribution around the notch can be quite intense as compared to the far field stress distribution. For a semi-infinitely long bar, moving further away from the notch results in a uniform stress distribution as if there was no notch. This behavior according to Neuber [1]

* Corresponding author. Tel.: +1-410-278-8753.

E-mail address: cyril.l.williams.civ@mail.mil

is referred to as the law of the stress gradient. The stress concentration for a single semi-elliptical surface notch in a bar under a state of uniaxial tension or bending can be approximated in terms of the notch depth (t) and notch root radius (ρ) using Equation 1(a) [2]. It is evident from Equation 1 that as t approaches ρ (a circular notch), the stress concentration approaches 3. This implies that the stress in the vicinity of the notch root is three times that of the nominal stress ($3\sigma_\infty$).

Because of the high stresses developed around a single notch in structural members, the resultant stress can often lead to a localized failure which eventually propagates into a global failure of the structural member in question. A clever way to avoid such localized failure is by minimizing the stress concentration in the vicinity of the notch root. This is often accomplished by introducing redundant notches of identical geometry equally spaced on either side of the principal notch as illustrated in Figures 1(c). The concept of introducing redundant notches in order to minimize the stress concentration is normally referred to as load relieving notches [1,2,3]. Fig. 1(d) represents a plate with circular holes loaded in tension perpendicular to the line of holes. The stress concentration for this case can be approximated using Equation 1(b) [2], where a , b , σ_{max} , and σ_∞ represent the diameter of the circular hole, spacing of the holes, maximum stress developed in the plate (location shown in the figure), and applied nominal stress respectively. It is evident from Equation 1(b) that for a constant hole diameter as b becomes infinitely large, the stress concentration (k_t) approaches $\sigma_{max}/\sigma_\infty$ and as b decreases, k_t decreases. This concept has been widely used in the design community to reduce the stress concentration introduced by principal notches on structural members. Also, the concept of load relieving notches has been validated by Hetenyi [9] using photoelastic experiments.

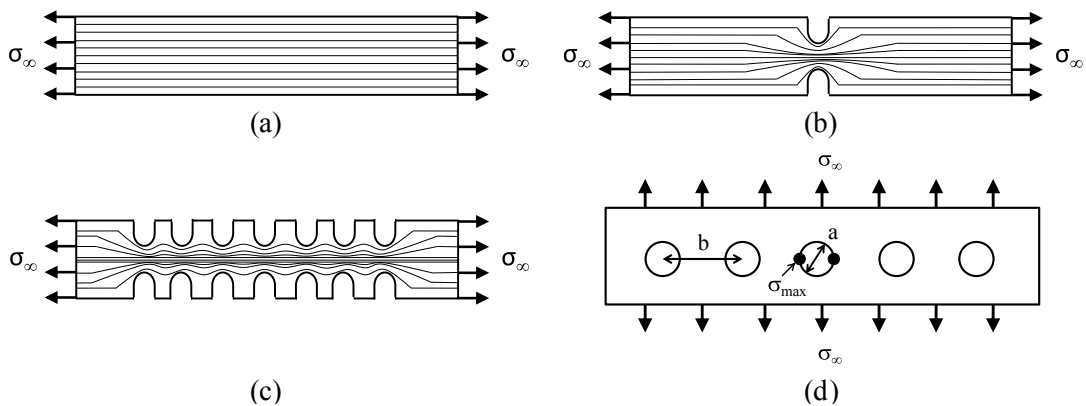


Fig. 1. (a) The stress field for an un-notched bar loaded in uniaxial tension, (b) the stress field around a single notch loaded in uniaxial tension, (c) the stress field around multiple notches loaded in uniaxial tension and (d) a plate with holes loaded in tension perpendicular to the line of holes.

$$K_t = 1 + 2\sqrt{\frac{t}{\rho}} \quad (1a)$$

$$K_t = \frac{\sigma_{max}}{\sigma_\infty} \left(1 - \frac{a}{b} \right) \quad (1b)$$

A theoretical background on the effects of load relieving notches was previously provided by Steinchen [6] and the reduction of stress concentration was defined as;

$$V(\Delta K_t) = \frac{K_t - (K_t)_{opt}}{K_t - 1} \quad (2)$$

where the change in stress concentration factor $\Delta K_t = K_t - 1$, $(K_t)_{opt}$ and K_t are the stress concentration factors with and without load relieving notches respectively. Note that as $(K_t)_{opt}$ approaches K_t , $V(\Delta K_t)$ tends to zero which implies that there is no reduction in stress concentration factor. A sample case for which $(K_t)_{opt}$ approaches K_t is when the separation distance between load relieving notches becomes quite large as compared to the radius of the notch. For such a case, the effect of load relieving notches diminishes.

The objective of this paper is to model and study the effects of load relieving notches subjected to shock loading using the standard plate impact test configuration with multiple notches at the back free surface of the target plate. The magnitude of the shock stress employed in this study was restricted to the weak shock regime (< 6 GPa) in order to avoid or delay complications such as jetting at the notch tip [10]. For this study, all the parameters such as shock stress, notch depth, notch

width, and specimen dimensions were kept constant while the notch spacing was varied. The resultant maximum tensile stress developed from interacting rarefaction waves was extracted for the different notch spacing and then compared.

2. Methodology

2.1. Simulation

All simulations were performed using version 8.1 of the CTH hydrocode [11] developed by Sandia National Laboratories. Two dimensional (2-D) simulations were performed using a plane-strain representation of the problem and taking advantage of symmetry such that only half of the flyer and target plates were modeled. The dimensions of the flyer plate in 2-D were 8 mm thick x 45 mm in diameter and details of the target plate are provided in Fig. 2 and Table 1. Note the difference in loading configuration between Fig. 1 and Fig. 2. The configuration in Fig. 2 was primarily chosen for this study because of its relative simplicity which enables us to interrogate the effects of notch spacing under shock loading conditions. Furthermore, the loading configurations shown in Fig. 1 cannot be attained under shock loading.

Both the 1100-O aluminum flyer and target plates were modeled using an elastic-perfectly plastic constitutive model and the Mie-Grüneisen Equation of State (EOS) was used to model the dilatational response of the plates using CTH library values for 1100-aluminum. The yield strength of the 1100-O aluminum was approximately 115.92 MPa.

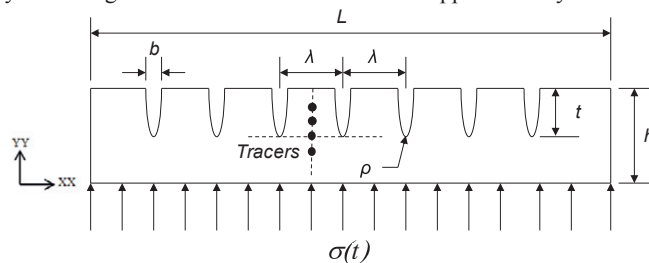


Fig. 2. Details of the shock loaded 1100-O aluminum target material with load relieving notches. $\sigma(t)$, λ , t , b , h , and L represents the shock stress, notch spacing, notch depth, notch width, specimen thickness, and specimen diameter.

Table 1. Dimensions for the shock loaded 1100-O aluminum target material.

Simulation #	# of Notches	λ (mm)	t (mm)	ρ (mm)	h (mm)	b (mm)	L (mm)
1	Baseline	-	-	-	12	-	45
2	Single	-	10	2	12	4	45
3	Three	12	10	2	12	4	45
4	Three	10	10	2	12	4	45
5	Five	8	10	2	12	4	45
6	Seven	6	10	2	12	4	45

According to Asay and Bertholf [10], for a yield stress-to-shock stress ratio of approximately 0.1 ($\sigma_y \sim 0.1\sigma(t)$) or greater, shock jetting can be considerably reduced or eliminated. Therefore, with this consideration in mind the flyer impact velocity was limited to approximately 500 m/s which corresponded to a shock stress of approximately 3.8 GPa for aluminum. Failure of the material was not studied and therefore was not modeled in this investigation. Four tracer particles were placed in a vertical array in between the central and first adjacent notch to capture the stress-time histories. As shown in Fig. 2, the tracers were placed even with the notch tip, 1 mm lower than the notch tip, 1 mm above the notch tip, and 2 mm above the notch tip (estimated spall plane for the baseline case). All simulations were terminated at 4.0 μ s because the maximum tensile stress developed in all the cases studied occurred prior to 4.0 μ s.

2.2. Plate Impact Experiments

Two plate impact experiments were conducted in order to validate the simulation results. A single stage 102 mm (slotted-bore) diameter gas gun at the shock physics laboratory, U.S. Army Research Laboratory (ARL), Aberdeen Proving Ground (APG) was used for both plate impact experiments. Both plate impact experiments were symmetric, implying that the impedance ($Z = \rho_0 C_0$, where ρ_0 and C_0 are the density and bulk sound speed respectively) of the flyer and target materials was the same. The sample (target) thickness was 12 mm and the diameter was 60 mm. The notch spacings for both experiments were 6 mm and 12 mm respectively representing the two extreme notch spacings. In order to mitigate spall failure within the sample, the flyer thickness was made similar to those of the target (12 mm thick) so that the estimated spall plane (assuming no notches) lies at the impact interface. The diameter of the flyer was 60 mm and the impact velocity for both experiments was restricted to approximately 500 m/s. A more detailed description of the plate impact technique employed in this research can be found in Williams et al. [12].

3. Results

Four plate impact simulations were performed to study the response of load relieving notches subjected to shock loading. Furthermore, two additional simulations were performed to study the response of the baseline case (no notch) and single notch case respectively. Selected stress-time histories obtained from CTH simulations representing the shock response of 1100-O aluminum for different notch spacing are shown in the following figures below. Figure 3(a) represents the baseline case for which there is no notch. At approximately 1 μs , two compression shock waves are shown traveling in opposite directions, one into the flyer and the other into the target. Further in time, both shock compression waves are reflected at the flyer and target free surfaces as rarefaction waves (not shown in the figure). In spall experiments involving ductile materials, both rarefaction waves at a later time will interact to form a tensile region in the target material. If the resulting tensile stress generated is greater than the threshold stress required for void nucleation, growth, and coalescence, then spallation of the target material occurs.

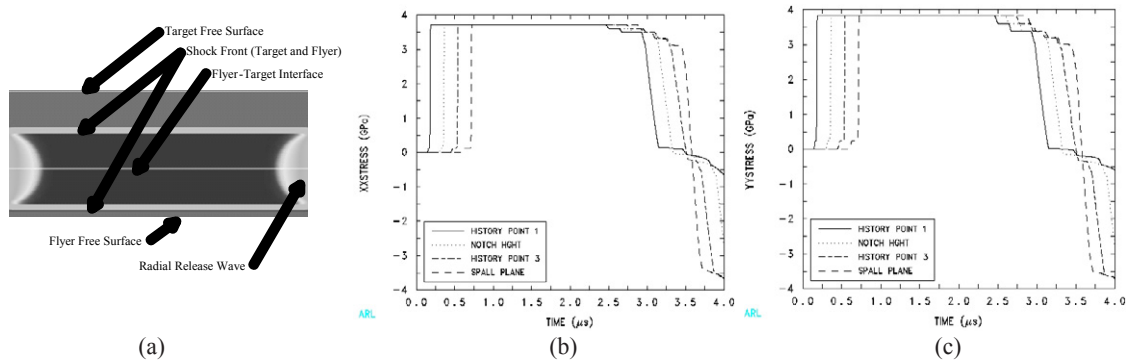


Fig. 3. (a) Simulation result for the baseline case with no notch at 1 μs , (b) and (c) are the resulting stress-time histories for various tracer locations up to 4 μs .

The baseline case represents the traditional test configuration of the spall plate impact technique albeit traditional spall fracture is not the primary interest in this study. However, it helps foster the understanding of notch effects. Also shown in Fig. 3(a) are two radial release waves originating from the edges of the flyer-target interface traveling towards the central region of both the target and flyer material. For all simulations performed, the pertinent information was acquired prior to the arrival of radial release waves at the tracer locations. Figure 3(b and c) are the stress-time histories in the through thickness (YY) and lateral (XX) directions for the baseline case acquired at the previously specified tracer locations. The times-of-arrival at the various tracer locations show a jump from ambient stress to a steady state shock stress of approximately 3.8 GPa in both directions and held at a predetermined pulse duration depending on the thickness of the flyer ($\sim 2.8 \mu\text{s}$ in this study). Following this, the material is then fully unloaded to ambient stress and then goes into tension in both (XX and YY) directions. Note that positive stress implies compression and negative stress implies tension in the stress-time plots. Also, note that all simulation results correspond to specific tracer locations; however, the maximum tensile stress developed in the material is extracted from the tracer positioned even with the notch tip.

Figure 4 shows both the simulation results and stress-time histories for the case with a single notch and the response is quite different from that of the baseline case. The compression shock wave traveling in the target material is reflected at the free surface of the notch as a rarefaction wave (circular) as shown in Fig. 4(a). The reflected wave from the semi-circular free surface of the notch consists of a leading longitudinal wave and a trailing shear wave. The expanding rarefaction waves eventually interact with the reflected planar rarefaction from the free surface of the flyer material resulting in a tensile region which can lead to material separation if the threshold for void nucleation, growth, and coalescence is met. Again, note the emergence of the radial release at the edge of the flyer-target interface. The stress-time histories for the single notch case at various tracer locations are shown in Fig. 4 (b and c).

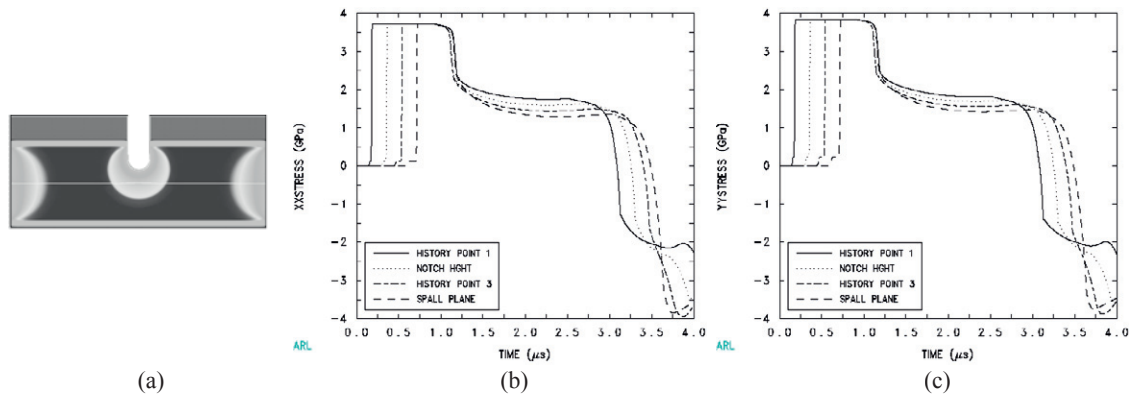


Fig. 4. (a) Simulation result for the single notch case at 1.2 μs , (b) and (c) are the resulting stress-time histories at various tracer locations up to 4 μs .

Figures 5 and 6 are simulation results and stress-time histories for the cases with 10 mm and 8 mm notch spacing respectively. For these cases, the plane shock compression wave in the target material is reflected from the free surfaces of the notches as rarefaction waves. The expanding circular rarefaction waves from adjacent notches interact to form tensile regions between notches as revealed in Figures 5(a) and 6(a). This behavior is captured quantitatively in the stress-time histories in Figures 5(b and c) and 6(b and c) in both the through thickness (YY) and lateral (XX) directions. The maximum tensile stress is the stress minimum developed between release and recompression of the material (the point at which the stress reverses from tension to compression). All data collected to analyze the effects of load relieving notches on the 1100-O aluminum subjected to shock wave loading were extracted prior to the arrival of the radial release waves emanating from the edges of the flyer-target interface. Therefore, tracers for all simulations were positioned close to the central notch to avoid rogue radial release waves. This is of utmost importance when extracting the resulting maximum tensile stress because after the arrival of the radial release waves, the resulting stress state becomes extremely complex for analysis.

4. Discussion

The maximum tensile stress extracted from the stress-time histories in both directions are plotted as a function of notch spacing in Fig. 7. As revealed in the figure, when the notch spacing is decreased, the maximum tensile stress developed in the material increases in both directions (XX and YY). This behavior is contrary to that of the quasi-static loading case [2] for which when the notch spacing was decreased, the stress decreases. Considering the two extreme notch spacings, the maximum tensile stress developed for the 6 mm spacing in the XX and YY directions were 0.95 GPa and 0.80 GPa respectively, while for the 12 mm spacing the maximum tensile stress developed was found to be 0.06 GPa in both directions. This represents approximately 94% and 93% reduction in maximum tensile stress in both the XX and YY directions respectively. Also, if the trend shown in Fig. 7 is extrapolated to represent a notch spacing far greater than 12 mm, then the maximum tensile stress will decay to approximately zero in both directions. This result will be analogous to the base line case previously described for which the stress jumps to steady state and then releases to ambient stress prior to the arrival of radial release waves. That is, for notch spacings greater than 12 mm, the effect of load relieving notches diminishes. However, in mechanical design, there are wide varieties of situations where design specifications limit the further increase in notch spacing. Therefore, this approach to studying the evolution of maximum tensile stress in structural members under shock loading can be readily employed by design engineers to reduce the maximum tensile stress developed between adjacent notches within the given specification.

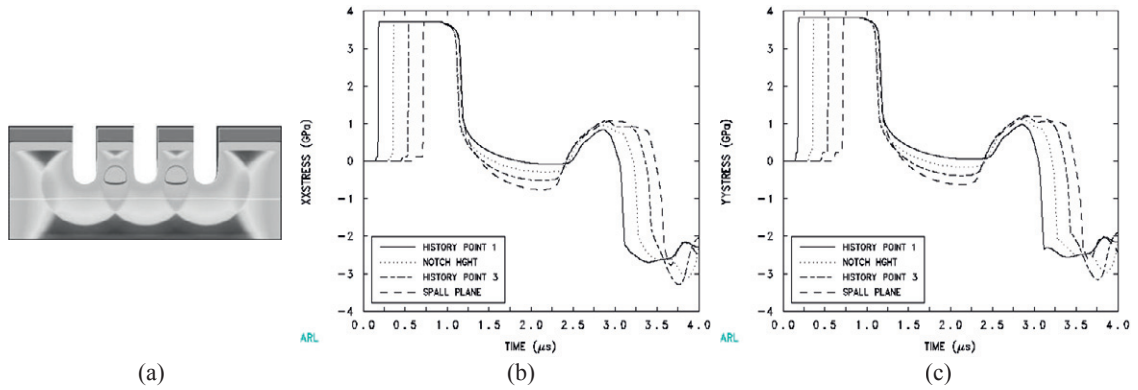


Fig. 5. (a) Simulation result for a target with three notches spaced 10 mm apart at 1.5 μs , (b) and (c) are the resulting stress-time histories at various tracer locations up to 4 μs .

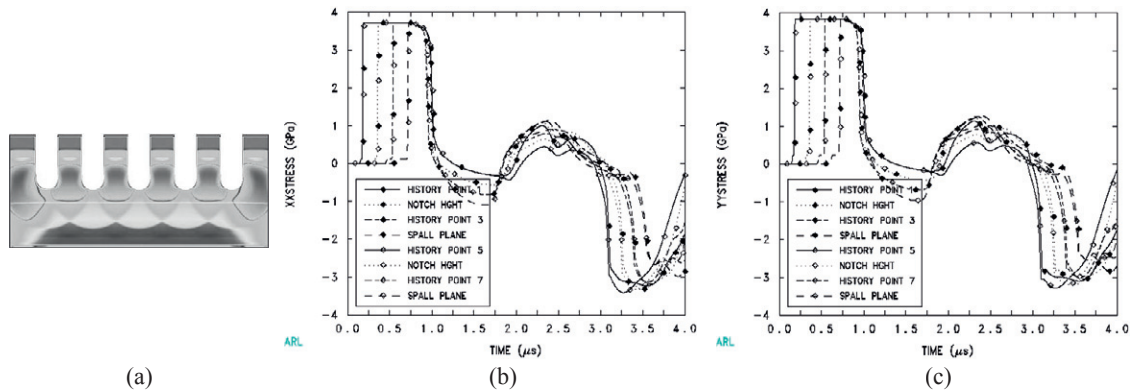


Fig. 6. (a) Simulation result for a target with five notches spaced 8 mm apart at 1.5 μs , (b) and (c) are the resulting stress-time histories at various tracer locations up to 4 μs .

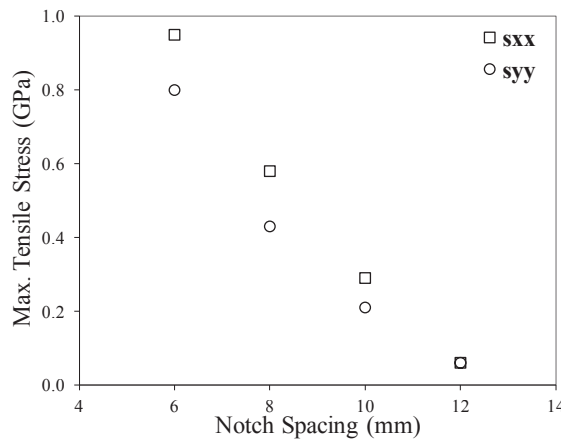


Fig. 7. The effect of notch spacing on the maximum tensile stresses (S_{xx} and S_{yy}) developed under shock loading conditions. S_{yy} represents the stress in the through thickness direction and S_{xx} represents the stress in the lateral direction.

The time taken to develop the maximum tensile stress was also plotted as a function of the notch spacing as shown in Fig. 8 and a linear relationship was observed. As the notch spacing is increased the time taken to develop the maximum tensile stress increases. This observation was expected, because for a constant velocity, the time required to develop the

maximum tensile stress must increase for an increase in notch separation distance. That is, the rarefaction waves from adjacent notches have to travel longer distances prior to collision. Increasing the notch separation distance allows for the head rarefaction to possibly catch up with the shock front and then attenuates it; note that the head of the rarefaction travels faster than the shock front. In other words, under similar conditions when two shocks of lower magnitude collide; the resultant tensile stress will be lower than that of two shocks with higher magnitude. Therefore, the magnitude of the reflected shock pulse decreases with increase in separation distance and consequently the resultant maximum tensile stress. This drop in peak shock stress with increase in distance is a possible attribute to the decrease in maximum tensile stress developed in the material.

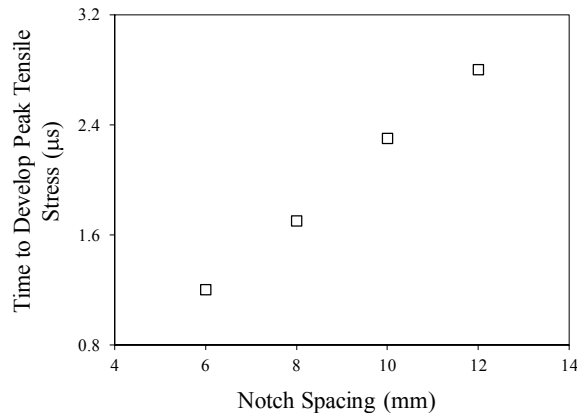


Fig. 8. The effect of notch spacing on the time taken to develop maximum tensile stress.

Simulation results were validated by plate impact experiments. Figures 9(a) represents micrographs of the sample shocked to approximately 3.8 GPa respectively. The notch spacing of the pre-shocked sample was 6 mm and the micrographs in the figure represent the front and back face of the sectioned sample respectively. Jetting is evident in both micrographs (denoted by the letters A and B); this observation is consistent with simulation results at times greater than 3.5 μs as shown in Fig. 9 (b). The micrographs also reveal a hairline macrocrack between two adjacent notches within the approximate region of maximum tensile stress. The macrocrack is aligned more or less orthogonal to the lateral tensile loading direction. However, for the post shocked sample with 12 mm notch spacing, no macrocracks were observed between the notches as evident from Fig. 10 (a). However, some damage was observed in the region of maximum tensile stress (denoted by the oval B). In addition, evidence of jetting was also observed in this case (denoted by the letter A) and a macrocrack crack was observed at the notched surface (denoted by C). These results are in reasonably good agreement with hydrocode simulations. It is noteworthy to point out that the nucleation and formation of macrocracks in the region of maximum tensile stress is strongly dependent on the shock stress. That is, macrocracks can develop with both 6 mm and 12 mm notch spacing, if the shock stress is strong enough. However, for this study a weak shock was employed to avoid severe jetting within the notch.

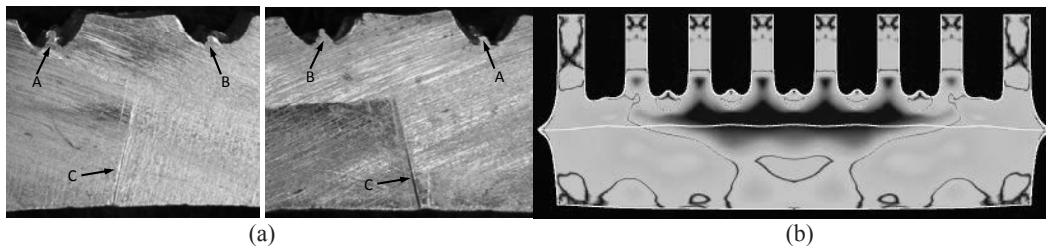


Fig. 9 (a). Optical micrographs of the post shocked sample with 6 mm notch spacing where A and B show evidence of jetting, and C denotes the hairline crack developed in the region of maximum tensile stress - both micrographs were obtained from opposite faces of the sample (b) simulation result show evidence of jetting at 4 μs .

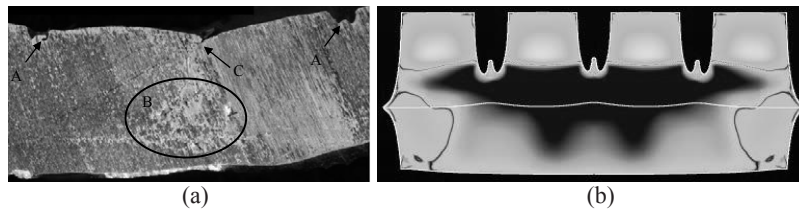


Fig. 10 (a). Optical micrograph of the post shocked sample with 12 mm notch spacing where A denotes evidence of jetting at both notches, B denotes a lightly damaged region, and C denotes a crack nucleated at the surface (b) simulation result show evidence of jetting at 4 μ s.

5. Conclusion

The hydrocode (CTH) was proven to be a credible tool for analyzing the non-linear response of 1100-O aluminum with load relieving notches subjected to shock wave loading. This approach can be an extremely useful tool for design engineers. The resulting maximum tensile stress developed between notches shows a strong dependence on notch spacing for the range studied. A 94% and 93% reduction in maximum tensile stress was observed in both the XX and YY directions respectively when the notch spacing was increased from 6 mm to 12 mm. When the maximum tensile stress developed from hydrocode simulations is extrapolated beyond 12 mm notch spacing, the result converges to that of the baseline case (a plate without a notch). Plate impact experimental results were in reasonably good agreement with those obtained from hydrocode simulations. A single hairline macrocrack was observed for the 6 mm notch spacing because of the high tensile stress developed, while some damage but no macrocrack was observed for the 12 mm notch spacing. Future hydrocode simulations and plate impact experiments are planned to further probe the response of load relieving notches subjected to oblique impacts (longitudinal and shear waves) and the effects of different notch geometries.

Acknowledgements

The authors are grateful to Dr. Steven Segletes for reviewing the manuscript and making meaningful suggestions. The authors also gratefully acknowledge the personnel at the Shock Physics Laboratory (ARL); Dr. Rich Becker for useful technical suggestions and test directors (Tim Cline and Codie Adams) for conducting the plate impact experiments.

References

- [1] Neuber, H., 1946. Theory of Notch Stresses. J. W. Edwards, Ann Arbor, Michigan.
- [2] Peterson, RE., 1953. Stress Concentration Design Factors. John Wiley & Sons, Inc.
- [3] Arola, D., Williams, CL., 2002. Estimating the Fatigue Stress Concentration Factor of Machined Surfaces. International Journal of Fatigue Vol. 24 (9), p. 923.
- [4] Mow, C., Pao Y., 1971. The Diffraction of Elastic Waves and Dynamic Stress Concentrations. United States Air Force Project Rand, R-482-PR.
- [5] Nakayama, N., Ohashi, M., Sano, T., Horikoshi, S., Takeishi, H., 1997. Dynamic Stress Concentration Factor in the Strip Plate with Fillet. J. Phys IV, France, 7.
- [6] Steinchen, WP., 1978. Experimental and Computer-Aided Investigations and Optimization of Stress Relieving Notches. Journal of Strain Analysis Vol. 13 (3), p. 149.
- [7] Shea, R., 1963. Dynamic Stress Concentration Factors. Watertown Arsenal Laboratories, Technical Report WAL TR 811.6/1.
- [8] Niethammer, RJ., Kim, KS., Ballmann, J., 1995. Numerical Simulations of Shock Waves in Linear-Elastic plates with Curvilinear Boundaries and Material Interfaces. International Journal of Impact Engineering, Vol. 16, No. 5/6, p.711.
- [9] Hetenyi, M., 1943. The Distribution of Stress in Threaded Connections. Proc. SESA, Vol. 1, No. 1, p. 147.
- [10] Asay, J., Bertholf, LD., 1978. A Model for Estimating the Effects of Surface Roughness on Mass Ejection from Shocked Materials. SAND78-1256.
- [11] McGlaun, JM., Thompson, SL., Elrick, MG., 1990. CTH: a three-dimensional shock wave physics code. International Journal of Impact Engineering, 10(1-4), pp. 351-360.
- [12] Williams, CL., Ramesh, KT., Dandekar, DP., 2012. Spall Response of 1100-O Aluminum, J. Appl. Phys. 111, 123528 (2012).

<u>NO. OF COPIES</u>	<u>ORGANIZATION</u>
1 (PDF)	DEFENSE TECHNICAL INFORMATION CTR DTIC OCA
1 (PDF)	DIRECTOR US ARMY RESEARCH LAB IMAL HRA
1 (PDF)	DIRECTOR US ARMY RESEARCH LAB RDRL CIO LL
1 (PDF)	GOVT PRINTG OFC A MALHOTRA
39 (PDF)	DIR USARL RDRL CIH C P CHUNG J KNAP T HARKINS RDRL WM P BAKER R DONEY B FORCH J MCCAULEY P PLOSTINS RDRL WML B I BATYREV B RICE D TAYLOR N WEINGARTEN RDRL WML H B SCHUSTER RDRL WMM J BEATTY RDRL WMM B G GAZONAS C RANDOW T SANO RDRL WMM E J SWAB RDRL WMM F M TSCHOPP RDRL WMM G J ANDZELM RDRL WMP D LYON S SCHOENFELD RDRL WMP B C HOPPEL D POWELL S SATAPATHY M SCHEIDLER T WEERISOORIYA

<u>NO. OF COPIES</u>	<u>ORGANIZATION</u>
	RDRL WMP C R BECKER S BILYK T BJERKE D CASEM J CLAYTON D DANDEKAR M GREENFIELD R LEAVY M RAFTENBERG S SEGLETES C WILLIAMS RDRL WMP E S BARTUS

INTENTIONALLY LEFT BLANK.